

Classical evolution of fractal measures on the lattice

N. G. Antoniou, F. K. Diakonou, E. N. Saridakis,* and G. A. Tsolias

Department of Physics, University of Athens, GR-15771 Athens, Greece

(Dated: March 31, 2022)

We consider the classical evolution of a lattice of non-linear coupled oscillators for a special case of initial conditions resembling the equilibrium state of a macroscopic thermal system at the critical point. The displacements of the oscillators define initially a fractal measure on the lattice associated with the scaling properties of the order parameter fluctuations in the corresponding critical system. Assuming a sudden symmetry breaking (quench), leading to a change in the equilibrium position of each oscillator, we investigate in some detail the deformation of the initial fractal geometry as time evolves. In particular we show that traces of the critical fractal measure can sustain for large times and we extract the properties of the chain which determine the associated time-scales. Our analysis applies generally to critical systems for which, after a slow developing phase where equilibrium conditions are justified, a rapid evolution, induced by a sudden symmetry breaking, emerges in time scales much shorter than the corresponding relaxation or observation time. In particular, it can be used in the fireball evolution in a heavy-ion collision experiment, where the QCD critical point emerges, or in the study of evolving fractals of astrophysical and cosmological scales, and may lead to determination of the initial critical properties of the Universe through observations in the symmetry broken phase.

I. INTRODUCTION

Chains of non-linear coupled oscillators are of fundamental nature: they provide a laboratory to explore the setup of thermodynamical properties through the microscopic dynamics in complex systems [1, 2, 3]. In addition, being the discrete version of field theories, they naturally emerge in any numerical study of the non-linear dynamics as well as statistical mechanics of classical fields [4]. One of the most important questions in the later case is to determine the conditions which can drive the evolving system towards a thermalized stationary state. In the early days Fermi, Pasta and Ulam [5] have obtained deviations, even for large times, from the naively expected equipartition of the energy among the different oscillators. Through the efforts to explain these results, it became clear that, for appropriate initial conditions, a variety of stable periodic solutions (breathers, solitary waves) [6], defined on the non-linear chain, exists. Therefore, the choice of the ensemble of the initial configurations strongly influences the long time behavior of the system dynamics. Recent works [3, 4] show that for a random ensemble of initial configurations a sufficiently large system relaxes to the usual equilibrium distribution, but the corresponding relaxation time strongly depends on the parameters of the theory. These studies include the case when a chain of oscillators is replaced by a multi-dimensional ($2 - D$ or $3 - D$) lattice [4]. In fact, when considering non-linear lattices in more than one dimensions, the thermalized equilibrium state can possess critical properties. The question of how critical properties can dynamically occur in a system of coupled oscillators is not yet fully understood. Some recent investigations [2] indicate that changes in the topological properties of the phase space of the considered system are induced by fine tuning the mean kinetic energy of the oscillators. The critical state, when formed, is associated with appropriately defined fractal measures on the non-linear lattice.

In the present work we investigate the scenario when such a critical state has already been formed and a sudden symmetry breaking drives the system apart from critical behavior. Furthermore, it is assumed that the time scale of the symmetry breaking process is much smaller than the relaxation time of the oscillator dynamics. Although we are concerned in the general case of the evolution of a set with fractal geometry, we focus in the large subclass where the corresponding measure is generated by a scalar field. In fact, the scalar field dynamics considered in this work, covers a large variety of phenomena with critical fluctuations which at equilibrium are described by the universality class of the $3 - D$ Ising model and its projections to lower dimensions. Hence, the above model is of great physical interest since it is realized in many different areas of physics. In a heavy-ion collision experiment, if the fireball passes near the QCD critical point it acquires critical correlations. The subsequent expansion and cooling induces a non-equilibrium evolution for the effective field equations of motion, which dilutes the initial fractality. The question is whether the corresponding relaxation time is long enough in order to acquire imprints of the initial critical state at the detectors

*Electronic address: msaridak@phys.uoa.gr

[7]. On the other hand, within the framework of scalar field dynamics, one can impose initial conditions associated with self-similar fluctuations of the inflationary field, and study their evolution as they grow and transform to the large-scale inhomogeneities of the observable Universe [8]. A similar approach, but with different dynamics, has been applied to the fractal-like structure of the Universe at large scales (star and galaxy clusters). The evolution in this case is crucial for the substructure survival or deformation [9, 10].

In order to implement the aforementioned scenario we will use the critical state as initial condition posed on the oscillators in the lattice. The corresponding fractal measure is generated through a suitable excitation of the oscillators. Contrary to the existing analysis of correlations and their evolution in a fractal lattice [11], our approach is closer to the conditions expected to occur in a real critical system where inhomogeneities in the order parameter density have a fractal profile embedded in a conventional space. The evolution of initial fractal measures has been studied both classically, in the context of reaction-diffusion models [12], as well as quantum-mechanically [13]. In the classical case an unconventional decay of correlations was observed, while in the quantum one the initial fractal dimension turns out to be a conserved quantity.

We investigate first the $1-D$ case of a nonlinear chain and then extend our treatment to lattices in higher dimensions. The $1-D$ example, although it cannot be directly related to a critical system in the absence of long ranged interactions, due to the no-go theorem of Peierls [14], it helps for the simpler illustration of the basic dynamical mechanisms which dominate the evolution of the system in the meta-critical phase. The extension to $2-D$ is straightforward using the insight gained by the $1-D$ model. The main finding of this work is a set of conditions which control both qualitatively and quantitatively the time-scale for which traces of the initial critical state, characterized by the fractal mass dimension, sustain. In addition, we show that this is a new time-scale not directly associated with the relaxation time towards the false vacuum. Our analysis shows that the fractal dimension, describing the geometry of the critical state, is a valuable observable which can be determined even in the symmetry broken phase, allowing for the calculation of critical exponents and consequently for the determination of the universality class of the occurring transition [15].

The paper is organized as follows: in section II we describe the dynamical model used in our analysis and we explain the algorithm used to generate the initial conditions. In section III we give the numerical solution of the equations of motion for the $1-D$ case as well as the observables which are relevant in quantifying the effect of the sudden symmetry breaking. To facilitate our analysis we first consider in subsection IIIa the harmonic chain, and in subsection IIIb we include non-linear chain interactions. In section IV we extend our study to $2-D$, discussing also the higher dimensional case. Finally in section V we present briefly our concluding remarks.

II. GENERATING A FRACTAL MEASURE IN A CHAIN OF NON-LINEAR OSCILLATORS

The considered dynamical system consists of a set of coupled oscillators located on an equidistant lattice. These oscillators are the discretized version of a self-interacting scalar field. In a simplified approach we investigate first the $1-D$ case when the oscillators are arranged in a closed chain. The Lagrangian of this system is taken as:

$$L = \sum_{i=1}^N \left\{ \frac{1}{2} \dot{\sigma}_i^2 - \frac{1}{4\alpha^2} \left[(\sigma_{i+1} - \sigma_i)^2 + (\sigma_i - \sigma_{i-1})^2 \right] - V(\sigma_i) \right\}, \quad (1)$$

where α is the lattice spacing and $V(\sigma_i)$ is the self-interaction term. The coupling term between the oscillators originates from the discretization of the spatial derivative term in the lagrangian density of a scalar field $\sigma(x, t)$, while the choice of the potential is adapted to the typical form for the description of spontaneous symmetry breaking in second order phase transitions.

We study the dynamics implied by eq. (1) using appropriate initial conditions $\{\sigma_i(0)\}$ in order to define a fractal measure on the $1-D$ lattice [20]. The construction of these configurations is based on a finite approximation to the $1-D$ Cantor dust with prescribed Hausdorff fractal dimension D_f [16, 17]. Although the construction algorithm for such a set is described in several textbooks on fractal geometry we also present it here briefly in order to be self-contained. The first step in the algorithm is the partition of the finite real interval $[0, 1]$ into three successive subintervals of sizes ℓ_1 , ℓ_2 and ℓ_3 , in ratios $\frac{\ell_1}{\ell_2} = \frac{r}{1-2r}$ and $\frac{\ell_2}{\ell_3} = \frac{1-2r}{r}$, where $r \in (0, \frac{1}{2})$, covering the entire set $[0, 1]$. The middle subinterval is called *trema* where the two others are called *precurds* [16]. At each step of the algorithm the trema is omitted, while the precurds are divided also in three subintervals with sizes fulfilling the same ratios as above. At the k -th stage of the algorithm there are 2^k precurds and $2^k - 1$ tremas. In the limit $k \rightarrow \infty$ we obtain a Cantor dust with fractal dimension $\log 2 / \log(1/r)$. Thus choosing $r = 2^{-1/D_f}$, we can practically construct a set with the desired fractal dimension D_f .

A finite approximation to the Cantor dust with dimension D_f can be obtained using the centers of the precurds $x_i^{(k)}$ ($i = 1, \dots, 2^k$) at the k -th algorithm step. This set can be easily embedded on a finite equidistant lattice using

the transformation $\nu_i^{(k)} = \left[\frac{d_{max}}{d_{min}} x_i^{(k)} \right] + 1$, where $d_{min} = \min_{i \neq j} |x_i^{(k)} - x_j^{(k)}|$ and $d_{max} = \max |x_i^{(k)} - x_j^{(k)}|$, and $[\cdot]$ denotes the integer part. Thus, the set of $\nu_i^{(k)}$ is a realization of the Cantor dust defined in the interval $(0, N\alpha]$, with $N = \left[\frac{d_{max}}{d_{min}} \right] + 1$. In this interval we can construct a density as:

$$\rho_C^{(k)}(y) = \frac{1}{2^k} \sum_{i=1}^{2^k} \delta(y - \nu_i^{(k)}). \quad (2)$$

The fractal properties of the set are quantitatively depicted in the scaling law:

$$M(\varepsilon) \sim \varepsilon^{D_f}, \quad (3)$$

where $M(\varepsilon)$ is the number of set points $\nu_i^{(k)}$ within a distance ε from any given reference point $\nu_j^{(k)}$ ($j \neq i$) belonging to the set.

Using the density (2) we can map the fractal geometry of the Cantor dust approximation to the non-linear oscillators on the lattice by assuming that the displacement of the ν -th oscillator is obtained through the integral

$$\sigma_\nu = \eta_\nu 2^k \int_{\nu-\delta/2}^{\nu+\delta/2} \rho_C^{(k)}(\xi) d\xi, \quad (4)$$

where η_ν is a random variable taking the values ± 1 with equal probability, $0 < \delta \ll 1$ and $\nu = 1, \dots, N$. With this choice it is straightforward to define a fractal measure on the oscillator chain through the obviously fulfilled property

$$m(\zeta) = \left\langle \sum_{\nu=\nu_i^{(k)}}^{\nu=\nu_i^{(k)}+\zeta} |\sigma_\nu| \right\rangle \propto \zeta^{D_f}, \quad (5)$$

where the average is taken over all $\nu_i^{(k)}$.

An example of a σ -field configuration is depicted in fig. 1 for $k = 11$. It must be noted that the number of sites in

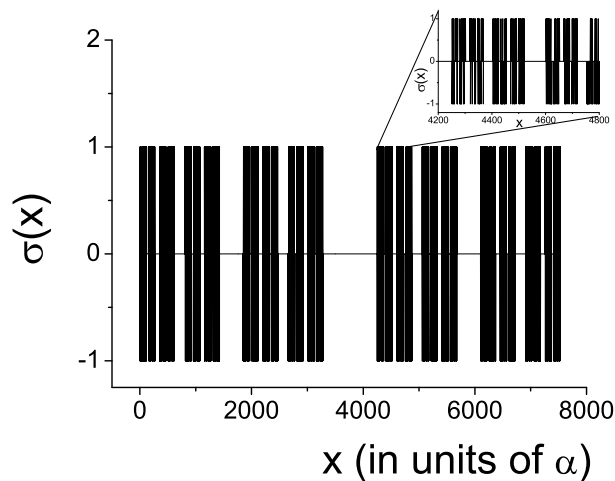


FIG. 1: The σ -field for a Cantor-like lattice of size $N = 18819$, obtained using $k = 11$ and $r = 2^{-6/5}$.

the obtained equidistant lattice ($N \approx 2 \times 10^4$) is much larger than that in the generating Cantor set (2^{11}). The inset is presented to illustrate the self-similarity of the set more transparently.

The constructed set of oscillators (σ -field) possesses the property (5), as can be seen in the log-log plot of $m(\zeta)$ versus ζ presented in fig. 2. The exponent D_f , i.e the fractal mass dimension, is equal to $5/6$ within an error of less than 1%.

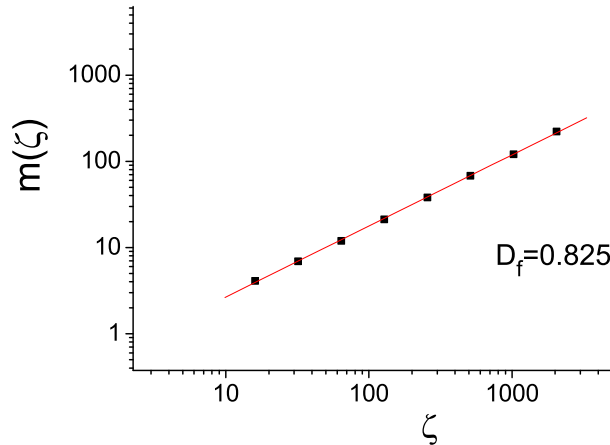


FIG. 2: $m(\zeta)$ vs ζ , in the constructed set of oscillators. The slope D_f is equal to $5/6$ within an error of less than 1%.

There are a few comments to be added concerning the connection of the constructed oscillator chain with critical phenomena. In fact the equilibrium position of the oscillators can be identified with the order parameter of an equivalent critical system, while the displacements σ_ν are associated with the fluctuations of the order parameter. Clearly, at the critical point the expected fluctuation pattern possesses fractal characteristics in close analogy to the measure (5) defined on the considered oscillator chain.

III. FRACTAL MEASURE DEFORMATION IN THE 1 - D CASE

In the previous section we determined the values of the scalar σ -field on the N lattice sites, in order to present fractal characteristics. That is, from the total of N oscillators we have displaced 2^k of them to the value ± 1 while keeping the rest to zero, in such a way that eq. (5) holds and the system possesses a fractal mass dimension D_f . We are interested in studying the evolution of this σ -configuration according to the dynamics determined by the Lagrangian (1), and especially we focus on the evolution of $m(\zeta)$. Before considering an anharmonic, in general, potential suitable to describe the aforementioned symmetry breaking (for example of fourth order), it is interesting to investigate the simple harmonic case where there is some analytic information, in order to acquire a better apprehension. However, even this simple model will reveal a rich and unexpected behavior.

A. Second order potential

We consider first the second order potential

$$V(\sigma) = \frac{\lambda}{4}(\sigma - 1)^2 - A\sigma, \quad (6)$$

where λ and A are the coupling parameters of our model. All the quantities (σ , λ , A , as well as the space-time variables) appearing above are taken dimensionless. The corresponding equation of motion for the i -th oscillator derived from eqs. (1) and (6) is:

$$\ddot{\sigma}_i = \frac{1}{\alpha^2}(\sigma_{i+1} + \sigma_{i-1} - 2\sigma_i) - \left[\frac{\lambda}{2}\sigma_i - \frac{\lambda}{2} - A \right]. \quad (7)$$

In order to solve it we use the leap-frog time discretization scheme, leading to:

$$\sigma_i^{n+2} = 2\sigma_i^{n+1} - \sigma_i^n + \frac{dt^2}{\alpha^2}(\sigma_{i+1}^{n+1} + \sigma_{i-1}^{n+1} - 2\sigma_i^{n+1}) - dt^2 \left[\frac{\lambda}{2}\sigma_i^{n+1} - \frac{\lambda}{2} - A \right], \quad (8)$$

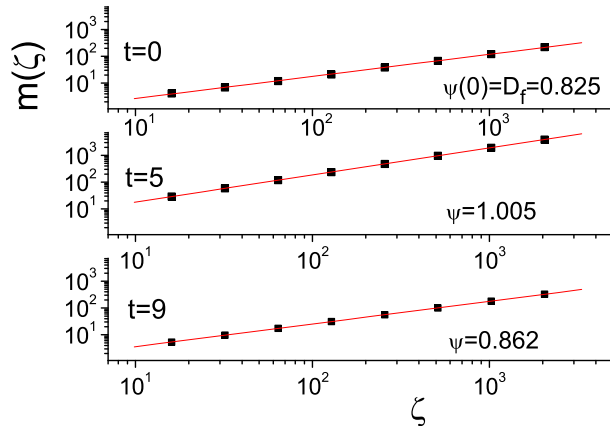


FIG. 3: $m(\zeta)$ vs ζ for three successive times, $t = 0$, $t = 5$ and $t = 9$, for $\lambda = 1$ and $A = 1$.

where α is the lattice spacing and dt is the time step. The upper indices indicate the time instants and the lower indices the lattice sites. As usual we perform an initial fourth order Runge-Kutta step to make our algorithm self-starting, and we impose periodic boundary conditions. The numerical integration results are not sensitive to the α and dt choice, provided that $dt \leq \alpha/2$.

Let us first assume zero initial kinetic energy, i.e. $\dot{\sigma}_i = 0$ for every lattice site, which physically is a strong requirement of equilibrium. We evolve the constructed fractal configuration, obtained using $k = 11$, according to (8) for various potential parameters. In fig. 3 we depict $m(\zeta)$ versus ζ for three successive times, $t = 0$, $t = 5$ and $t = 9$, for $\lambda = 1$ and $A = 1$. Initially the slope ψ is the fractal mass dimension D_f . Here we have chosen $D_f = 5/6$. As we can see, the initial fractal geometry is completely lost at $t = 5$. However, at $t = 9$ it is almost re-established.

Let us explore this remarkable result further. In the upper graphs of fig. 4 we present the evolution of the mean field value $\langle \sigma(t) \rangle$ for three λ and A cases. In the lower ones we show the corresponding evolution of the slope $\psi(t)$ of $m(\zeta)$ versus ζ (each $\psi(t)$ value obtained through a linear fit). First of all, the spatial mean field value $\langle \sigma(t) \rangle$ oscillates around the potential minimum $\sigma_{min} = 1 + \frac{2A}{\lambda}$ with constant amplitude as expected. Secondly, one oscillator moving in the potential (6) has the period $T = \frac{2\pi\sqrt{2}}{\sqrt{\lambda}}$, and this holds equally well for $\langle \sigma(t) \rangle$ too, due to the synchronization of the dominating zero background [18].

We observe that the exponent $\psi(t)$ rapidly reaches the embedding dimension value 1, but it reacquires a value close to the initial one periodically. It is easy to see that this (partial but clear) re-establishment of the initial fractal geometry happens at times where $\langle \sigma(t) \rangle$ returns to its starting point, which is the lower turning point of the oscillations. In the case we are looking at, this starting point corresponds to $\langle \sigma(0) \rangle \approx 0$ (since only a small fraction of sites is displaced to ± 1 while the others form a zero background) and to $\dot{\sigma}_i(0) = 0$ for every oscillator. Therefore, the explanation for this behavior is induced easily. Indeed, initially only the discrete set of oscillators displaced to ± 1 contributes to the integral (5), while the zero background adds with zero effect. As the system of coupled oscillators evolves in the potential (6), this zero background is excited and its non-zero but trivial contribution to (5) sufficiently overcomes that of the initial ± 1 's and consequently deforms completely the fractal geometry. However, we expect a simultaneous return of this background to zero (synchronization) since the energy transfer between the different oscillators takes place through the spatial derivative (which is small since the displacement to ± 1 is not large compared to the potential minimum) and therefore only the zeros close to the initial ± 1 's will return to a different value. Moreover, this behavior is amplified by the initial zero kinetic energy for all oscillators, which strengthens homogeneity. As a result, at times where $\langle \sigma(t) \rangle$ and the zero background return to the lower turning point, the system re-exhibits a power law behavior in $m(\zeta)$ with exponent close to the initial one, i.e. to the fractal mass dimension $D_f = 5/6$. Each re-appearance of the initial fractal geometry will survive as long as the system stays close to its lower turning point, therefore the corresponding interval will be larger for smoother potentials at their minimum. This effect can be weakly seen comparing the lower left and right plots of fig. 4. Lastly, due to the non-trivial excitation of the zeros in the neighborhood of the initial ± 1 's, which number increases monotonically as time passes, every partial re-establishment of the initial fractal geometry will possess slightly larger exponent than the previous one. This behavior is observed in fig. 4, where the $\psi(t)$ value at the minima increases successively. Therefore, we expect that the dynamics will totally deform the original fractality in the end.

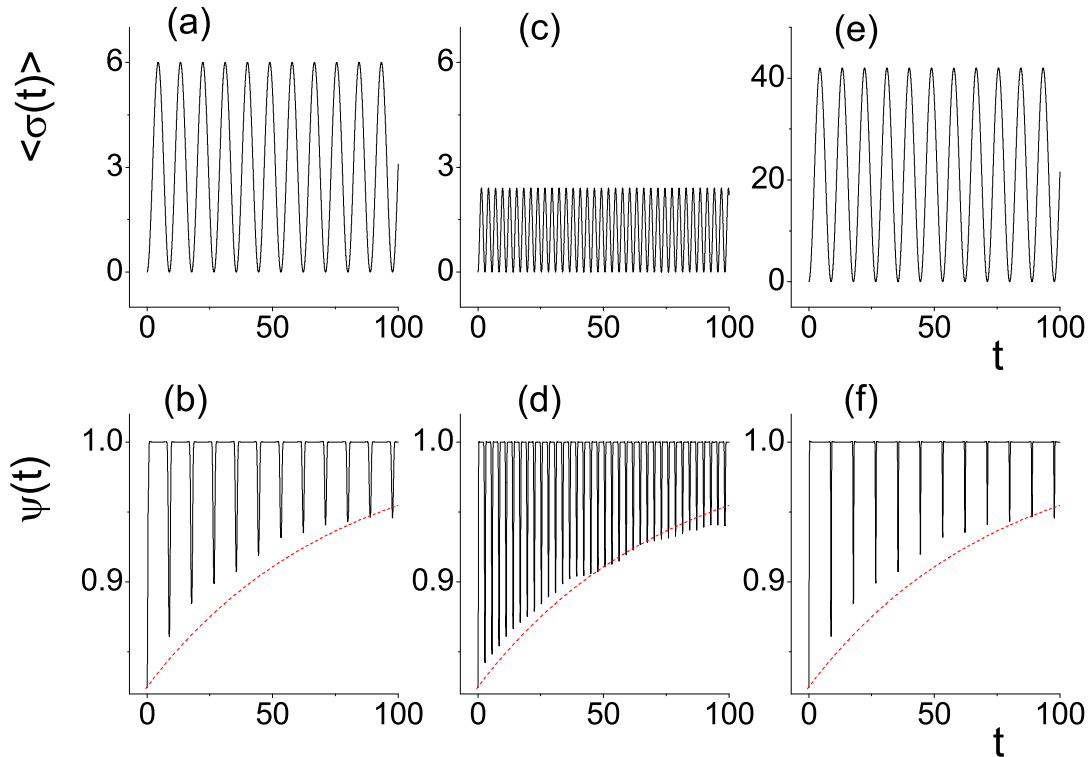


FIG. 4: $\langle \sigma(t) \rangle$ and $\psi(t)$ evolution for $\lambda = 1$ and $A = 1$ ((a) and (b) plots), for $\lambda = 10$ and $A = 1$ ((c) and (d) plots) and for $\lambda = 1$ and $A = 10$ ((e) and (f) plots). The dashed line in the lower graphs marks the $F(t) = 1 - (1 - \psi(0))e^{-qt}$ curve, with $q = 0.013$.

A supporting argument for the cogitation analyzed above is the calculation of $\Delta E(t) = \sqrt{\sum_i^N [E_i(t) - E_i(0)]^2}$, which provides a measure for the divergence of the oscillators' total energies from their initial values. In fig. 5 we plot $\Delta E(t)$ for $\lambda = 10$ and $A = 1$ case. As we observe, it presents minima for the same times as $\langle \sigma(t) \rangle$ and $\psi(t)$, therefore the partial re-appearance of the fractal geometry happens when the oscillators acquire energies close to their initial ones. However, $\Delta E(t)$ cannot describe the mixing of energy between the different oscillators.

There are two time scales in the reappearance phenomenon. The first, naming τ_1 , is the period of the partial re-establishment of the initial fractal mass dimension. It coincides with the oscillations period as we have already mentioned. The second, τ_2 , is the time scale which determines the complete deformation of the initial fractal geometry. We quantify an estimation of τ_2 by assuming that the ratio of two successive variations of $\psi(t)$ at the corresponding minima is constant. If ψ_l denote these successive minima and $t_l = l\tau_1$ the corresponding successive times, this natural assumption reads:

$$\frac{\psi_{l+2} - \psi_{l+1}}{\psi_{l+1} - \psi_l} = C. \quad (9)$$

This finite difference equation has the solution:

$$\psi_l = 1 - (1 - \psi(0)) e^{-qt_l}, \quad (10)$$

if $C = e^{-q\tau_1}$, where we have added the necessary terms in order to get correct values for $l = 0$ ($\psi(0)$) and for $l \rightarrow \infty$ ($\psi(t_l) \rightarrow 1$). Therefore, we determine τ_2 in terms of the exponent q as $\tau_2 \approx 5/q$, since the characteristic time is $1/q$ and for $t = 5/q$ the deviation from the embedding dimension is considered as completely lost, falling below the threshold value of 10^{-2} (in close analogy with capacitor discharge in electronics). The approximation (9) reproduces

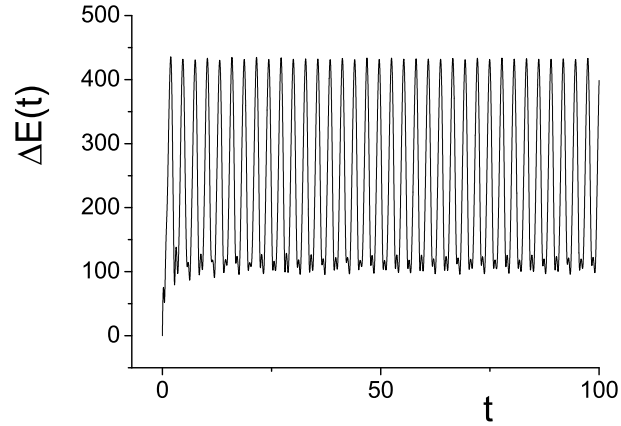


FIG. 5: $\Delta E(t)$ for $\lambda = 10$ and $A = 1$. The minima coincide with those of $\langle \sigma(t) \rangle$ and $\psi(t)$.

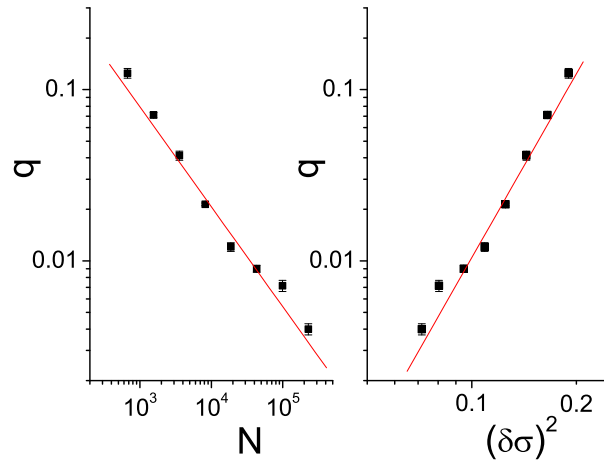


FIG. 6: On the left we show the exponent q defined in eq. (10) versus total lattice site number N , for $\lambda = 1$ and $A = 1$. On the right we show q versus the initial variation of the field values $(\delta\sigma)^2$, calculated for the different N values of the left plot. The solid lines mark exponential fits.

very well the exact ψ_l behavior, as can be observed in fig. 4 where we display, with the dashed line, the analytical estimation (10) for $q = 0.013$. Indeed, q offers a measure of the deformation of the initial fractal geometry, and in the following we investigate numerically its dependence on the various model parameters.

Firstly, q , i.e. τ_2 , is completely independent from λ and A , contrary to τ_1 which (coinciding with the oscillation period) depends on λ . The constant value of q for different A and λ , is a result of the increase of the oscillation frequency combined with a compensating decrease of the difference $\psi_{l+1} - \psi_l$. The corresponding $q - \lambda$ and $q - A$ plots are trivial horizontal lines.

On the left plot of fig. 6 we depict the dependence of q on the total number of lattice sites N , for $\lambda = 1$ and $A = 1$. Note that increasing k in the construction of the Cantor 2^k -point set, we result to a much more rapidly growing equidistant lattice (the points in fig. 6 correspond to a successive increase of k from 7 to 13). It is clear that q decreases exponentially with N , therefore the deformation becomes weaker. The explanation is straightforward since by increasing the number of the Cantor points (which will form the ± 1 's in the equidistant lattice) we need much more sites with zero value. In other words, the measure of the ± 1 's relatively to the zero background decreases with

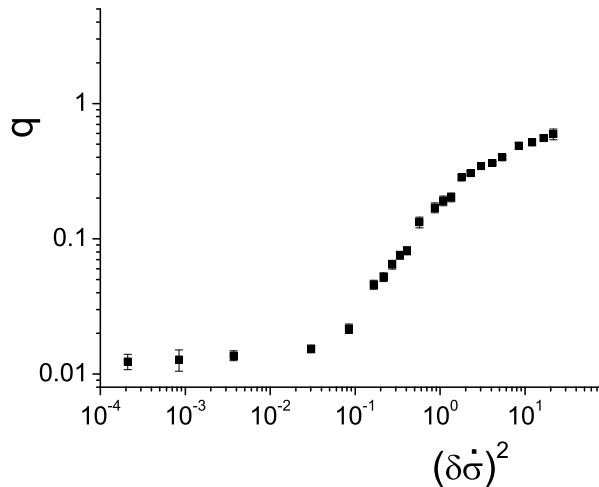


FIG. 7: Exponent q versus initial variation of time derivatives of the field values $(\delta\dot{\sigma})^2$, for $N = 18819$ (2^{11} Cantor points), for $\lambda = 1$ and $A = 1$.

N . Due to the influence of this background to the re-appearance phenomenon (larger times needed for the mixing of the oscillators through the spatial derivative) the deformation becomes weaker with N , i.e q decreases. Finally, it is obvious that in an infinite system the initial fractal geometry will be periodically deformed and re-established for infinite time ($q \rightarrow 0$, i.e $\tau_2 \rightarrow \infty$ for $N \rightarrow \infty$), since in this case the initial measure of the ± 1 's is zero and therefore infinite time is needed for the mixing and de-synchronization of the zero background.

On the right graph of fig. 6 we show the dependence of q on the initial variation of σ -field, calculated by $(\delta\sigma)^2 = \langle \sigma^2 \rangle - \langle \sigma \rangle^2 = \sum_i \sigma_i^2 / N - (\sum_i \sigma_i / N)^2$ at $t = 0$, for the different N values used in the left plot. The initial variation of the σ -field, reflecting the domination of the homogenous zero background, affects the deformation exponent q . Larger initial $(\delta\sigma)^2$ values correspond to zero background with smaller measure relatively to the ± 1 's, and therefore to weaker re-appearances, i.e to larger q 's. On the other hand, for $N \rightarrow \infty$ $(\delta\sigma)^2 \rightarrow 0$, the measure of the ± 1 's becomes zero, and the re-appearance phenomenon holds for ever ($q \rightarrow 0$, i.e $\tau_2 \rightarrow \infty$).

Another possibility could be to change the initial $(\delta\sigma)^2$ by displacing randomly all the oscillators from their constructed values, while keeping N constant. However, we avoid doing so since this procedure alters the initial fractal mass dimension. Instead, we may perturb randomly the initial time derivatives and investigate the effect of the variation of the initial kinetic energies on q . In fig. 7 we present the dependence of q on the variation of $\dot{\sigma}_i$ at $t = 0$, given by $(\delta\dot{\sigma})^2 = \langle \dot{\sigma}^2 \rangle - \langle \dot{\sigma} \rangle^2 = \sum_i \dot{\sigma}_i^2 / N - (\sum_i \dot{\sigma}_i / N)^2$, for $N = 18819$ (2^{11} Cantor points), in the $\lambda = 1$, $A = 1$ case. Indeed we observe a significant increase of q for larger $(\delta\dot{\sigma})^2$ as expected, due to the de-synchronization of the zero background, i.e the initially zero oscillators are excited and mixed due to their different kinetic energies too, apart from their coupling to the ± 1 's. Mind that the turning point is not zero any more and $\langle \sigma(t) \rangle$ moves to negative values, too. Finally, note that additionally to this $\dot{\sigma}(0)$ perturbation, there is always a constant initial $(\delta\sigma)^2$ present, resulting from the ± 1 's ($(\delta\sigma)^2 \approx 0.1$ in this specific case), which cannot be removed. Therefore, the stabilization of q for sufficiently small $(\delta\dot{\sigma})^2$ is due to the overcoming effect of $(\delta\sigma)^2$ comparing to that of $(\delta\dot{\sigma})^2$.

Finally, a quantitative measure concerning the aforementioned dynamics is the Lyapunov exponent. Following [2] we can calculate it analytically in this simple second order potential case. The constant curvature of the external potential leads to Lyapunov exponent exactly equal to zero, which according to our analysis can be related to $\lim_{N \rightarrow \infty} q$. However, a proof of this statement goes beyond the scope of the present work.

B. Fourth order potential

After analyzing the simple second order potential case, which revealed an interesting behavior though, we extend our investigation to the fourth order model which will give rise to non-linear equations of motion. The potential has

the form

$$V(\sigma) = \frac{\lambda}{4}(\sigma^2 - 1)^2 - A\sigma. \quad (11)$$

Inspired by the σ -model we assume that the Z_2 symmetry ($\sigma \rightarrow -\sigma$) is broken only through a linear term, setting the coefficient of the cubic term in the potential to zero. The equations of motion derived from eqs. (1) and (11) is:

$$\ddot{\sigma}_i = \frac{1}{\alpha^2}(\sigma_{i+1} + \sigma_{i-1} - 2\sigma_i) - [\lambda\sigma_i^3 - \lambda\sigma_i - A], \quad i = 1, \dots, N \quad (12)$$

which are solved using the leap-frog time discretization algorithm given in the previous subsection.

We evolve the constructed fractal configuration according to (12), assuming zero initial kinetic energy, for various potential parameters. In fig. 8 we draw the potential for three λ and A cases and in fig. 9 the corresponding evolution of $\langle\sigma(t)\rangle$ and $\psi(t)$. The spatial mean field value $\langle\sigma(t)\rangle$ oscillates around the potential minimum, which now is one of

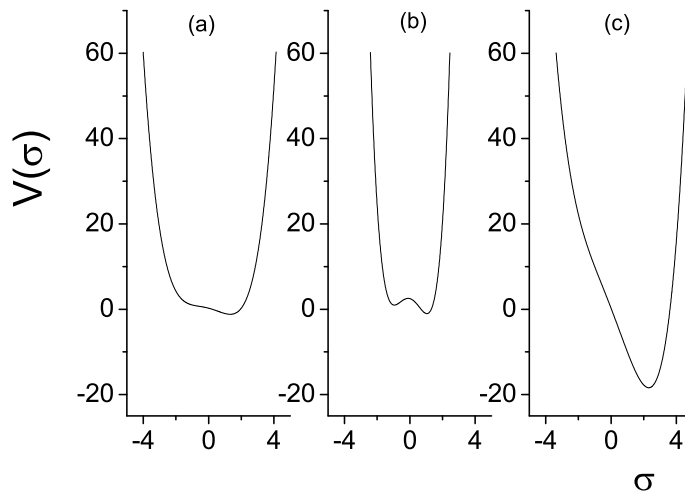


FIG. 8: Potential (11) for $\lambda = 1$ and $A = 1$ (plot (a)), for $\lambda = 10$ and $A = 1$ (plot (b)) and for $\lambda = 1$ and $A = 10$ (plot (c)).

the three roots of $V'(\sigma) = \lambda\sigma^3 - \lambda\sigma - A = 0$. Depending on λ and A we can have two minima and a maximum (middle plot of fig. 8), one minimum and one saddle point, or just one minimum (left and right plots of fig. 8). Contrary to the second order case of fig. 4, the oscillation amplitude decreases with time due to the anharmonic dynamics. However, the amplitude attenuation weakens with increasing lattice size N and for an infinite system it remains constant.

As we observe in fig. 9, the periodical partial re-appearance of the initial fractal mass dimension at times when $\langle\sigma(t)\rangle$ has a minimum, holds similarly to the harmonic case. Firstly, in this anharmonic case, as $\psi(t) \rightarrow 1$ the power-law form of $m(\zeta)$ is slightly distorted at large ζ values due to the finite system size. Consequently, the power-law fit leads occasionally to effective $\psi(t)$ slightly greater than 1. To correct this behavior, one could restrict the fit to smaller ζ values (worsening statistics) or go to significantly larger lattices (huge computational times). Indeed, in fig. 10 we present $\psi(t)$ evolution for a Cantor-like lattice of size $N = 228208$, obtained using $k = 14$, where the tendency of $\psi(t)$ to approach the limiting value ($\psi(t) \rightarrow 1$) becomes obvious. However, since this effect does not influence the re-appearance phenomenon and its characteristics, we will ignore it in the following analysis. Secondly, the time scale τ_1 , which determines the period of the re-appearance, coincides with the oscillation period T . It cannot be calculated analytically and in fig. 11 we depict its dependence on λ and A found numerically. Thirdly, the computation of $\Delta E(t)$ leads to similar to the second order case results, that is it possesses minima simultaneously with $\langle\sigma(t)\rangle$ and $\psi(t)$.

Continuing we study the dependence of the exponent q of eq. (10), which quantifies the gradual permanent deformation of the initial fractal geometry, on the various parameters. Note however that in general in this fourth order potential case the upper envelope of the $\psi(t)$ graph is more complex. In fig. 12 we present q versus lattice site number N (left plot), and versus the corresponding initial variation $(\delta\sigma)^2$ (right plot). Its behavior is similar to the second order case of fig. 6 and the interpretation is the same. However, the corresponding q values seem to be slightly increased, that is the anharmonic dynamics deforms the initial fractal geometry earlier. The explanation

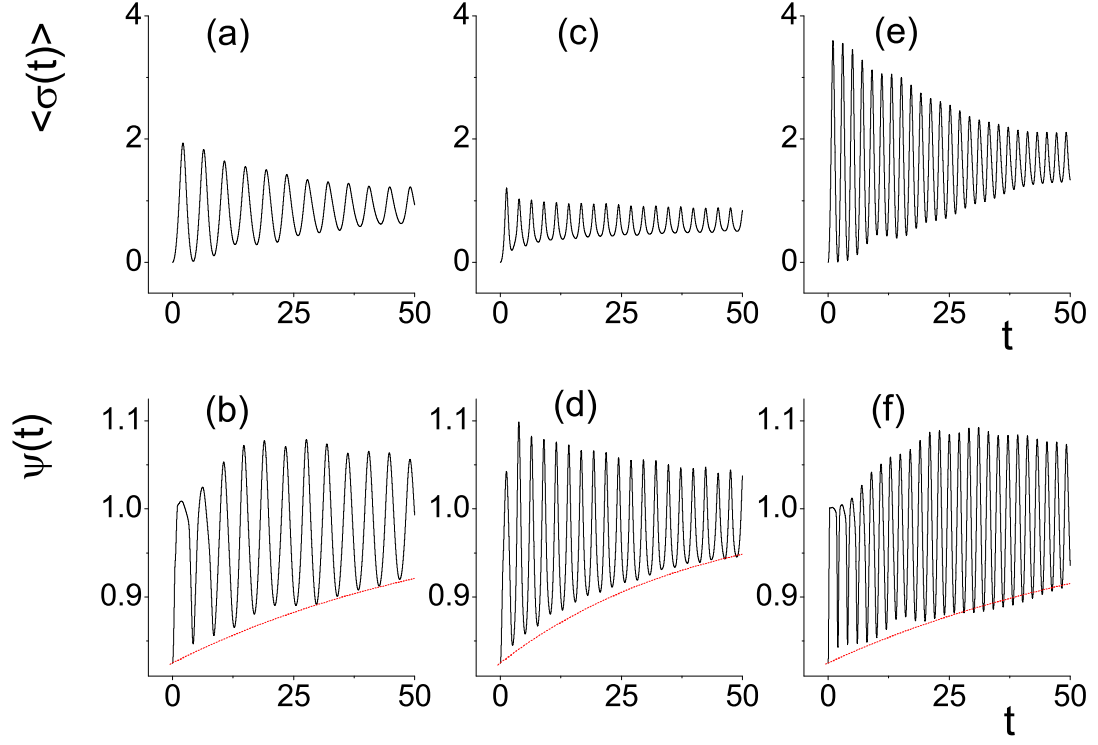


FIG. 9: $\langle \sigma(t) \rangle$ and $\psi(t)$ evolution for $\lambda = 1$ and $A = 1$ ((a) and (b) plots), for $\lambda = 10$ and $A = 1$ ((c) and (d) plots) and for $\lambda = 1$ and $A = 10$ ((e) and (f) plots), in the fourth order potential case. The dashed line in the lower graphs marks the $F(t) = 1 - (1 - \psi(0))e^{-qt}$ curve, with $q = 0.016$, $q = 0.024$ and $q = 0.014$, respectively.

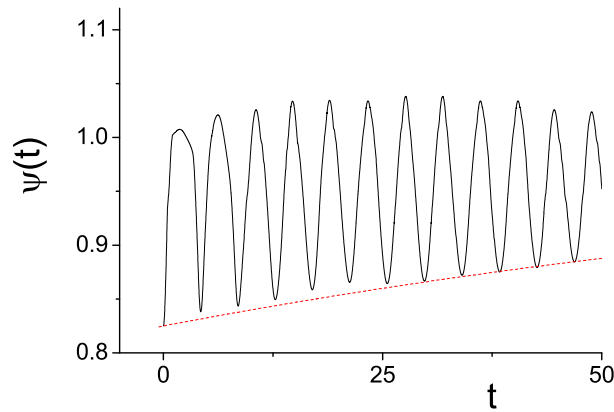


FIG. 10: $\psi(t)$ evolution for $\lambda = 1$ and $A = 1$ in the fourth order potential case, for a Cantor-like lattice of size $N = 228208$, obtained using $k = 14$. The dashed line marks the $F(t) = 1 - (1 - \psi(0))e^{-qt}$ curve, with $q = 0.0089$. The effective exceeding of 1 is decreased due to the increased lattice size.

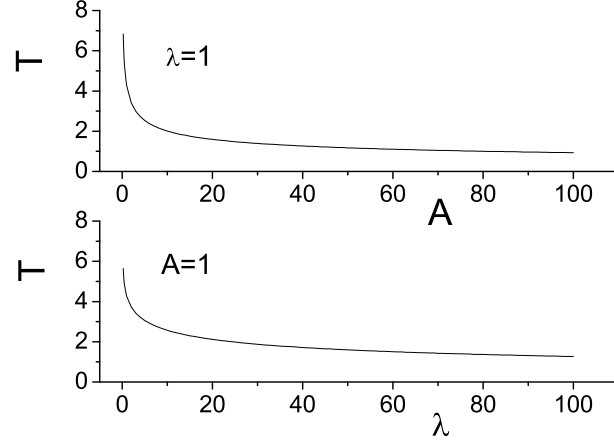


FIG. 11: Dependence of oscillations period T , which coincides with time scale τ_1 , on A and λ in the fourth order potential case.

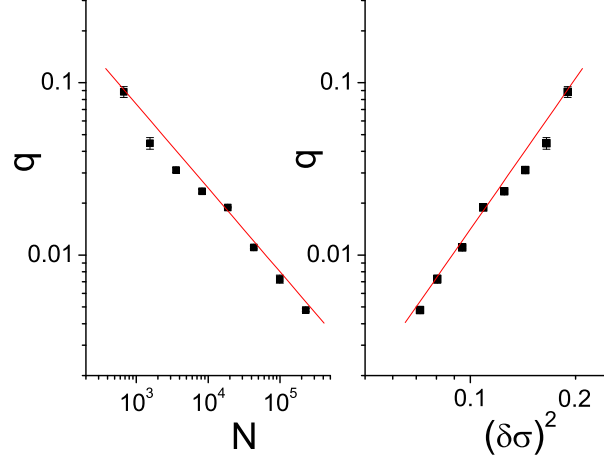


FIG. 12: On the left, the exponent q and its errors versus total lattice site number N , for $\lambda = 1$ and $A = 1$ in the fourth order potential case. On the right, q versus the initial variation of the field values $(\delta\sigma)^2$, calculated for the different N values of the left plot. The solid lines mark exponential fits.

of this behavior is the decreasing oscillations amplitude of this case (see fig. 9). Indeed, the system lower turning point moves gradually to larger values, i.e $\langle\sigma(t)\rangle$ does not return to zero and the initially zero background remains excited, thus spoiling the fractal mass dimension. The permanent oscillators displacement from zero is an additional mechanism of the fractality deformation in a finite system, apart from the mixing and de-synchronization caused by the partial derivative. Its effect weakens with increasing N , since the amplitude attenuation weakens too, as we have already mentioned.

The amplified deformation rate can be deduced also from fig. 13, where we depict the dependence of q on the initial variation of σ_i . It resembles the corresponding fig. 7 of the harmonic case but now q is significantly larger, especially for large $(\delta\sigma)^2$. Therefore, the increased initial kinetic energy interferes intensely with the complex fourth order dynamics, leading to a deformation of the initial fractality at significantly smaller times.

The main difference between fourth and second order cases, is the effect of λ and A on q . Contrary to the previous harmonic potential, where $q - \lambda$ and $q - A$ plots are trivial horizontal lines, in fig. 14 we show these graphs for the case in hand. We elicit that q increases almost algebraically with λ while it decreases with A in a more complex way.

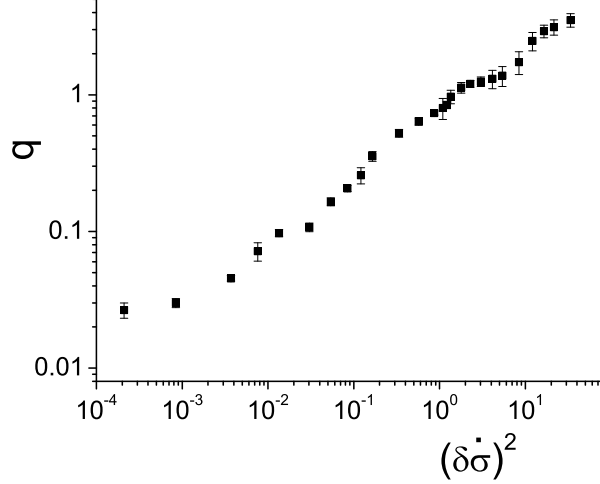


FIG. 13: Exponent q versus initial variation of time derivatives of the field values $(\delta\dot{\sigma})^2$, for $N = 18819$ (2^{11} Cantor points), for $\lambda = 1$ and $A = 1$ in the fourth order potential case.

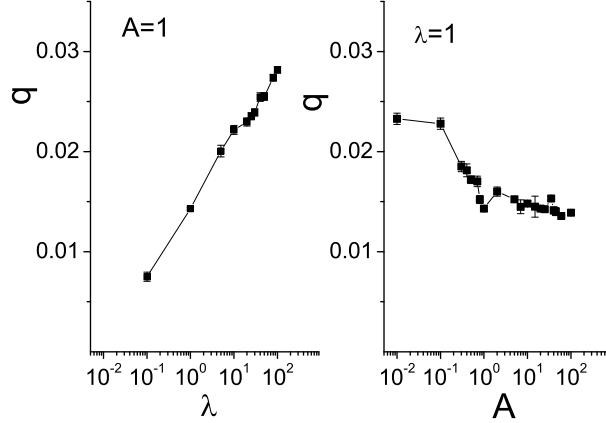


FIG. 14: q dependence on λ (left plot) and A (right plot) in the fourth order potential case, for $N = 18819$ (2^{11} Cantor points).

Although variation of λ seems to be slightly more important than that of A , both have less influence on q than N and $\dot{\sigma}_i$.

A possible explanation of this dependence of q on λ and A , could be the corresponding Lyapunov exponent. For the fourth order potential this exponent cannot be calculated analytically. We estimate it semi-analytically following [2], and we find that for finite N it is not zero anymore, but it takes a small non-zero value depending on the potential parameters, especially on its curvature, i.e on λ . However, even in this anharmonic case, the Lyapunov exponent seems to tend to zero for larger N , therefore an infinite system will possess the re-appearance phenomenon for infinite time ($q \rightarrow 0$, i.e $\tau_2 \rightarrow \infty$ for $N \rightarrow \infty$), consistently with fig. 12.

IV. TWO AND HIGHER DIMENSIONAL EVOLUTION

It is necessary to investigate the validity of the allegation described above in higher dimensional systems, where critical behavior can naturally arise. Keeping as a central observable of interest for the critical system the fractal

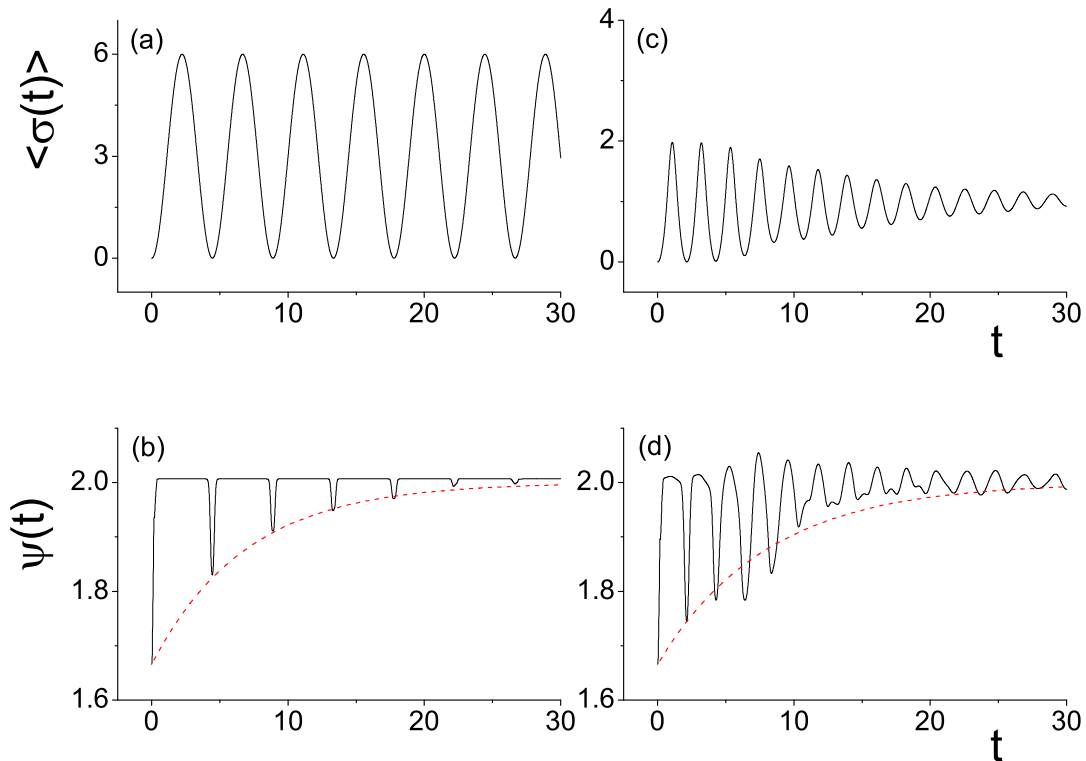


FIG. 15: $\langle\sigma(t)\rangle$ and $\psi(t)$ evolution for $\lambda = 1$ and $A = 1$, for the second order potential ((a) and (b) plots), and for the fourth order one ((c) and (d) plots). The dashed line in the lower graphs marks the $F(t) = 2 - (2 - \psi(0))e^{-qt}$ curve, with $q = 0.14$ and $q = 0.13$ respectively.

geometry of the clusters formed at the critical point, it is possible to model, in a simplified manner, the critical system with an ordinary geometrical set possessing the appropriate fractal mass dimension. In fact we can construct a set with dimension D_f embedded in a D -dimensional space, by taking the Cartesian product of $1 - D$ sets, generated by the procedure described in section II, each one having fractal mass dimension D_f/D [19]. For simplicity we consider here the $2 - D$ case, leading to a $N_1 \times N_2$ lattice where the field values are the products of the corresponding one-dimensional ones, thus resulting to $2^{k_1} \times 2^{k_2} \pm 1$'s. As a concrete example, following the steps of section II we produce a 1551×1551 lattice arising from the Cartesian product of two 2^8 Cantor sets, each one possessing fractal mass dimension $5/6$. The set of lattice sites with non-vanishing field values is a finite realization of a fractal set with dimension $5/3$ embedded in a two dimensional space.

It is straightforward to generalize the equations of motion (7), (12), for the second and fourth order potential cases respectively. Initial equilibrium corresponds to field configuration with zero kinetic energy, similarly to the $1 - D$ analysis. The evolution of the system is depicted in fig. 15 for $\lambda = 1$ and $A = 1$. We show the mean displacement $\langle\sigma(t)\rangle$ (averaged over the lattice), as well as the running mass dimension $\psi(t)$. We observe the same phenomenon of the partial re-establishment of the initial fractal geometry every time $\langle\sigma(t)\rangle$ approaches its lower turning point. The time scale τ_1 of the re-appearance period coincides with that of the oscillations, and the envelope of the minima of $\psi(t)$ has an exponential form with exponent q similarly to the $1 - D$ case, suggesting that the analysis of the previous section is also valid in this case. It is clearly seen in fig. 15 that $\psi(0)$ equals $5/3$, and $\psi(t)$ reaches successively the embedding dimension value 2 as expected. However the exponent q is almost one order of magnitude larger, leading to the conclusion that the higher dimensional dynamics deforms the initial fractal geometry earlier.

The same procedure can be easily extended to three dimensions. However since the lattice site number increases rapidly with increasing dimension we have to use a very coarse-grained approximation of the initial Cantor set in order to acquire plausible computational evolution times.

V. SUMMARY AND CONCLUSIONS

In the present work we have investigated the evolution of a fractal set resembling the order parameter clusters formed at the critical point of a macroscopic system. Our analysis is based on a simplified description of the critical system, restricted to the reproduction of the correct fractal mass dimension. We assumed initial equilibrium and we explored the variation of this appropriately defined fractal mass dimension with time. We have found that the initial fractal geometry is being deformed and partially re-established periodically, at times when the mean field value returns to its lower turning point. The origin of this effect is made more transparent in a harmonic $1 - D$ model. For a complete study we investigated the influence of anharmonic interactions as well as initial deviations from equilibrium, on the time scales determining the re-appearance phenomenon. We derive an analytical expression describing, to a sufficient accuracy, the value of the running fractal mass dimension $\psi(t)$ at the re-appearance times, and we show that the re-appearance frequency coincides with that of the oscillations. The total duration of the re-establishment process is inversely proportional to a characteristic exponent q , which depends on various parameters of the model. In particular q is a decreasing function of the total lattice size N , the initial field variation $(\delta\sigma)^2$ and the initial time derivative variation $(\delta\dot{\sigma})^2$. Therefore in an infinite system the initial fractal mass dimension re-appears for ever. The only qualitative difference of the harmonic and anharmonic analysis is the q dependence on the potential parameters λ and A in the fourth order case.

The same treatment can be followed in higher dimensional ($D \geq 2$) systems, too. In these more relevant, for the simulation of real critical systems, cases, we observe a similar behavior which can be explained in an analogous manner. The only quantitative difference is that q increases significantly with D . Therefore, the partial re-appearance of the initial fractal geometry seems to be a robust property of the evolution of critical systems, rendering the corresponding fractal dimension a significant observable which can be determined even in the symmetry broken phase. This in turn allows for the calculation of critical exponents and the determination of the universality class of the occurring transition. Our analysis is of interest for the study of the fireball evolution in a heavy-ion collision experiment, when the system at some intermediate stage passes through the QCD critical point, and the main question is whether imprints of the transient critical state can sustain for sufficiently large times in order to be observed at the detectors [7]. Similarly, it could be applied to the primordial fractal fluctuations of the inflationary field in order to investigate their evolution to the present large scale inhomogeneities and, with appropriate modifications, to the evolution of astrophysical fractals, such as star and galaxy clusters, to determine their deformation scales.

Acknowledgements: We thank V. Constantoudis and N. Tetradis for useful discussions. One of us (E.N.S) wishes to thank the Greek State Scholarship's Foundation (IKY) for financial support. The authors acknowledge partial financial support through the research programs "Pythagoras" I and II of the EPEAEK II (European Union and the Greek Ministry of Education) and "Kapodistrias" of the University of Athens.

-
- [1] M. Toda, *Theory of nonlinear lattices*, Springer Verlag (1989).
 - [2] L. Caiani, L. Casetti, C. Clementi and M. Pettini, Phys. Rev. Lett. **79**, 4361 (1997).
 - [3] G. Parisi, Europhys. Lett, **40** (4), 357 (1997).
 - [4] G.F. Bonini, C. Wetterich, Phys. Rev. **D 60**, 105026 (1999)[arXiv: hep-ph/9907533]; G.F. Bonini, C. Wetterich, Nucl.Phys. **B 587**, 1-3, 403 (2000) [arXiv:hep-ph/0003262]; S. Juchem, W. Cassing, C. Greiner, Phys. Rev. **D 69**, 025006 (2004)[arXiv:hep-ph/0307353].
 - [5] E. Fermi, J. Pasta, S. Ulam, Los Alamos Rpt. LA-1940, 20 (1955); also in "Collected Works of E. Fermi", University of Chicago Press, Vol II (1965).
 - [6] J. Ford, Phys. Rep. **213**, 271 (1992).
 - [7] N. G. Antoniou, F. K. Diakonou, E. N. Saridakis, [arXiv:hep-ph/0610382].
 - [8] C. J. A. P. Martins and E. P. S. Shellard, Phys. Rev. D **73**, 043515 (2006) [arXiv:astro-ph/0511792].
 - [9] S. P. Goodwin and A. P. Whitworth, Astron. Astrophys. **413**, 929 (2004) [arXiv:astro-ph/0310333v1].
 - [10] Y. Baryshev and P. Teerikorpi, Bull. Spec. Astrophys. Obs. Russian Academy of Sciences, vol. 59, 2005 [arXiv:astro-ph/0505185].
 - [11] U. M. B. Marconi and A. Petri, Phys. Rev. E **55**, 1311 (1997).
 - [12] P. A. Alemany, J. Phys. A **30**, 3299 (1997).
 - [13] D. Wójcik, I. Bialynicki-Birula and K. Życzkowski, Phys. Rev. Lett. **85**, 5022 (2000).
 - [14] R. E. Peierls, *Surprises in Theoretical Physics*, Princeton University Press, Princeton, NJ (1979).
 - [15] R. B. Stinchcombe, *Order and Chaos in Nonlinear Physical Systems*, Plenum Press, New York (1988).
 - [16] B. B. Mandelbrot, *The Fractal Geometry of Nature*, W. H. Freeman and Company, New York (1983).
 - [17] T. Vicsek, *Fractal Growth Phenomena*, World Scientific, Singapore (1999).

- [18] L. M. Pecora and T. L. Carroll, Phys. Rev. Lett. **64**, 821 (1990); G. Hu, J. Xiao, J. Yang, F. Xie and Z. Qu, Phys. Rev. E **56**, 2738 (1997); A. Pikovsky, M. Rosenblum and J. Kurths, *Synchronization: A Universal Concept in Nonlinear Science*, Cambridge University Press, New York (2002).
- [19] K. Falconer, *Fractal Geometry: Mathematical Foundations and Applications*, John Wiley & Sons, West Sussex (2003).
- [20] In fact an ideal fractal in the mathematical sense cannot be defined on a discrete space. However, physical fractals are always defined between two scales and therefore can be embedded in a lattice.